Comparing Impacts of Satellite Data Assimilation and Lateral Boundary Conditions on Regional Model Forecasting: A Case Study of Hurricane Sandy (2012)

TONG ZHU

CIRA/Colorado State University, Fort Collins, Colorado, and NOAA/NESDIS/STAR/JCSDA, College Park, Maryland

SID AHMED BOUKABARA

NOAA/NESDIS/STAR, and NOAA/NESDIS/STAR/JCSDA, College Park, Maryland

KEVIN GARRETT

Riverside Technology, Inc., Fort Collins, Colorado, and NOAA/NESDIS/STAR/JCSDA, College Park, Maryland

(Manuscript received 19 April 2016, in final form 24 September 2016)

ABSTRACT

The impacts of both satellite data assimilation (DA) and lateral boundary conditions (LBCs) on the Hurricane Weather Research and Forecasting (HWRF) Model forecasts of Hurricane Sandy 2012 were assessed. To investigate the impact of satellite DA, experiments were run with and without satellite data assimilated, as well as with all satellite data but excluding Geostationary Operational Environmental Satellite (GOES) Sounder data. To gauge the LBC impact, these experiments were also run with a variety of outer domain (D-1) sizes. The inclusion of satellite DA resulted in analysis fields that better characterized the tropical storm structures including the warm core anomaly and wavenumber-1 asymmetry near the eyewall, and also served to reduce the forecast track errors for Hurricane Sandy. The specific impact of assimilating the GOES Sounder data showed positive impacts on forecasts of the storm minimum sea level pressure. Increasing the D-1 size resulted in increases in the day 4/5 forecast track errors when verified against the best track and the Global Forecast System (GFS) forecast, which dominated any benefits from assimilating an increased volume of satellite observations due to the larger domain. It was found that the LBCs with realistic environmental flow information could provide better constraints on smaller domain forecasts. This study demonstrated that satellite DA can improve the analysis of a hurricane asymmetry, especially in a shear environment, and then lead to a better track forecast, and also emphasized the importance of the LBCs and the challenges associated with the evaluation of satellite data impacts on regional model prediction.

1. Introduction and motivation

It has been demonstrated by many studies that satellite data have positive impacts on global numerical weather prediction (NWP) through the combined use of many newly available satellite observations and advanced data assimilation (DA) techniques (Andersson 2001; Bouttier and Kelly 2001; Simmons and Hollingsworth 2002; Zapotocny et al. 2007). Joo et al. (2013) found that satellite data accounted for 64% of the short-range global forecast error reduction, with the remaining 36% coming from the assimilation of surface-based observation types in the Met Office global NWP system.

Regional modeling systems have been widely used for short-range forecast and regional climate modeling. However, the impacts of any physical scheme, advanced DA techniques, and new satellite data are difficult to evaluate in the regional NWP models, mainly because of the influence of the lateral boundary conditions (LBCs). The sensitivity to LBCs is widely acknowledged in the regional climate modeling community, and it is suggested that the use of too small or too large of a model domain should be avoided (Larsen et al. 2013). Chikhar and Gauthier (2015) showed that the model was very sensitive to the imposed LBCs in the Canadian Regional

Corresponding author e-mail: Dr. Tong Zhu, tong.zhu@noaa.gov

DOI: 10.1175/WAF-D-16-0077.1

Climate Model. Nadeem and Formayer (2015) found that the domain size of the high-resolution Regional Climate Model (RegCM3) had a major impact on climate simulations and noted that direct nesting with a reasonable domain size was the most adequate method for reproducing precipitation over the European Alps.

The impact of the LBCs on short-range regional model forecasts is also complex. Warner et al. (1997) gave a comprehensive review on LBCs as a basic and potentially serious limitation to regional NWP and provided guidelines for minimizing the negative effects of LBCs. The use of satellite data in regional short-range forecast studies has yielded positive impacts (Zapotocny et al. 2005, Pu et al. 2009), as well as mixed results (Xu et al. 2009; Schwartz et al. 2012; Steeneveld et al. 2015). In a 30-day period of 24- and 48-h WRF-ARW forecast experiments over southwest Asia, Xu et al. (2009) found that the forecast errors were reduced to some degree over some of the areas of study by the Gridpoint Statistical Interpolation (GSI) assimilation of satellite data, but the improvement was very limited for the diurnal variation of the forecast. Schwartz et al. (2012) reported that assimilating microwave radiances with a limited-area ensemble adjustment Kalman filter (EAKF) system resulted in better intensity forecasts of tropical cyclones, but no substantial impact on tropical cyclone track forecasts, and the impacts on precipitation forecasts were mixed. Steeneveld et al. (2015) revealed that using a larger WRF Model domain over the Netherlands resulted in more scattered radiation fog than was found when working with a small domain. The results with the smallest domain represented the reality of radiation fog distribution.

The purpose of this study is to evaluate the impacts on tropical cyclone forecasts from satellite DA, particularly the assimilation of the Geostationary Operational Environmental Satellite (GOES) Sounder data, using the Hurricane Weather Research and Forecasting (HWRF) Model. In the current global GSI employed in the Global Forecast System (GFS), a 145-km horizontal resolution thinning grid is used for most of satellite radiance data. However, a 60-km thinning grid is used in the GSI/HWRF system, which could benefit from the higher spatial resolution of GOES Sounder data. The size of the domain in regional forecast models not only has a direct impact on the number of satellite observations assimilated, but also determines the LBCs to be imported from the global model. We will investigate the impacts of domain size changes on the track and intensity forecasts of a tropical cyclone.

Hurricane Sandy is chosen for this study not only because it was the second-costliest hurricane to impact the United States since 1900 (Blake et al. 2013), but also because of its unique characteristics from a research point of view (Galarneau et al. 2013; Zhu and Weng 2013; Magnusson et al. 2014). Sandy has been designated as the largest Atlantic storm on record (a diameter of over 1500 km). The unique track and storm structure of Sandy have been widely attributed to the interaction of the storm with large-scale weather patterns (McNally et al. 2014). Their study demonstrated that the polar-orbiting satellite data had played an important role in the successful prediction of this event by the European Centre for Medium-Range Weather Forecasts (ECMWF), a global NWP model, forecast 7 days in advance.

In this study, we will first give a brief description of the setup of the GSI and HWRF systems, along with the design of the experiments in section 2. The experiment results, including GSI analysis, satellite DA impacts, and the comparison of satellite DA and LBC impacts, will be presented in section 3. Section 4 provides summary and discussion.

2. Methodology

a. The GSI and HWRF system

In this study, the GSI/HWRF system obtained from the Developmental Testbed Center's (DTC) fiscal year 2013 (FY13) trunk version 3.5a is used to perform satellite data assimilation and create the forecast of Hurricane Sandy. The triply nested HWRF is configured using 27, 9, and 3 km, respectively, for the outermost (D-1), intermediate (D-2), and innermost (D-3) domains (Zhang et al. 2011; Tallapragada et al. 2014). The inner domains are two-way nesting domains and are designed to follow the projected path of the storm. There are 43 hybrid vertical levels with the model top at 50 hPa. A vortex initialization (Liu et al. 2012), including storm relocation, vortex specifying, and storm size and intensity corrections, is performed over a domain that extends slightly beyond the intermediate domain, which is then merged with the background fields, and followed finally by the GSI analysis.

The GSI is a three-dimensional variational data assimilation (3DVAR) system. The description of the GSI system can be found in Wu et al. (2002). The key aspect of the GSI is that it formulates the analysis in model grid space, which allows for more flexibility in the application of the background error covariances and makes it straightforward for a single analysis system to be used across a broad range of applications, including both global and regional modeling systems and domains (Kleist et al. 2009). In the original FY13 HWRF system setup, GSI is applied to only conventional observation assimilation (e.g., radiosondes; dropsondes; aircraft

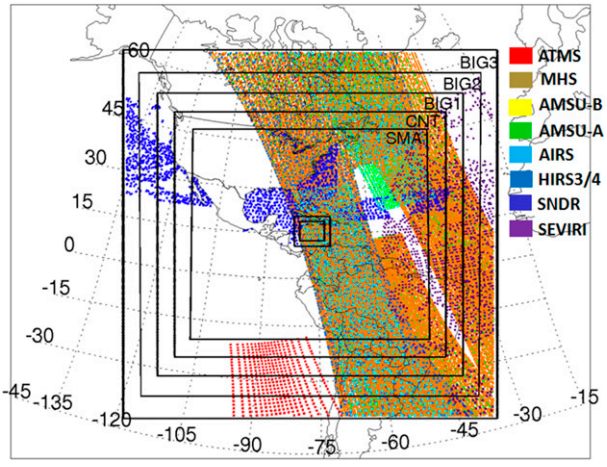

FIG. 1. HWRF domain-1 sizes for five experiments (SMA, CNT, BIG1, BIG2, and BIG3), and the data coverage of satellite observations from eight types of sensors at 1800 UTC 22 Oct 2012. The most inner two small domains are the two-way nested movable D-2 and D-3.

reports; land, ship, and buoy observations; and satellite retrievals). In this study, the GSI assimilation is also applied to satellite radiances for the experiments over the HWRF D-1 region, and the 60-km thinning grid is used. The global GFS analysis field is used as the background field during the first HWRF cycle of each experiment and, then, to avoid the double use of data, the 6-h HWRF forecasts are employed as the background fields for the subsequent GSI data assimilation cycles.

b. Experiment configuration

Two groups of experiments have been designed: one without satellite DA and the other with satellite DA. To investigate the sensitivity of the LBC effect, the experiments are run with five different D-1 sizes. In the original FY13 HWRF setup (CNT1), the sizes of the three nested domains are 216 × 432 grid points for D-1, 88 × 170 grid points for D-2, and 180 × 324 grid points for D-3. As shown in Fig. 1 and Table 1, the D-1 size is increased each time by about 700 km in both the x and y directions starting from a smaller than FY13 HWRF setup domain, called the SMA1 domain, and then increased to domains we call CNT1, BIG1, BIG2, and BIG3. The D-2 and D-3 sizes are kept unchanged for all of the experiments. In addition to the five experiments with satellite data assimilated and five experiments without satellite data assimilated, each with varying sizes of D-1, another experiment was performed to examine the impact of GOES Sounder data. In this experiment, all satellite data are assimilated as in the control run except for the GOES Sounder data (radiance and atmospheric motion vector). For each of above 11 experiments, there are a total of twenty 5-day HWRF forecast cycles, starting every 6 h from 1800 UTC 22 October 2012 and continuing through 1200 UTC 27 October 2012.

Figure 1 also illustrates an example of the coverage of the satellite radiance data that are assimilated in the second group of experiments for the 1800 UTC 22 October 2012 analysis cycle. These satellite observations are routinely assimilated in the 2012 global GSI analysis system, and include the Advanced Microwave Sounding Unit-A (AMSU-A) on board the *NOAA-15*, *-18*, and *-19* and *Aqua* satellites; the Advanced Microwave Sounding Unit-B (AMSU-B) on board *NOAA-17*; the Microwave Humidity Sounder (MHS) on board *NOAA-18* and *-19*; the Advanced Technology Microwave Sounder (ATMS) on the *Suomi National Polar-Orbiting Partnership* (*SNPP*), the Atmospheric Infrared Sounder (AIRS) on *Aqua*; the High Resolution Infrared Radiation Sounder (HIRS) on *NOAA-17* and *-19*; the Spinning Enhanced Visible and Infrared Imager (SEVIRI) on the *Meteosat Second Generation-9* satellite (*MSG-9*); and the *GOES-13/15* Sounder. As shown in Fig. 2, the sensors with the largest volume of observations assimilated are AIRS and AMSU-A over the BIG3 domain. However, the data availability of the polar-orbiting satellite data across 1 day of assimilation cycles is not evenly distributed; the largest volumes of data are available at 0600 and 1800 UTC, especially for the AIRS data. On the other hand, the observation numbers from two geostationary satellite sensors are evenly distributed during the four analysis cycles per day, but contribute just 5.7% of the total assimilated satellite observations.

3. Results

a. GSI analysis results

Among Hurricane Sandy's unique features are the asymmetric structures during the middle part of its life cycle from 25 to 26 October 2012. During this time period, Sandy encountered and interacted with an upper-level trough and attendant midlatitude cold front approaching from the northwest. The large vertical wind shear weakened Sandy and created asymmetric structures within the storm. The strong environmental shear and asymmetric pattern of Sandy lasted for about 2 days (Blake et al. 2013; Zhu and Weng 2013). It was found that the assimilation of satellite radiance data produced analysis fields that captured the asymmetric pattern and provided improved initial conditions for the HWRF forecasts.

To quantitatively examine the evolution of Sandy's asymmetric structure, we performed a fast Fourier transform (FFT) of the GSI-analyzed wind field from the WCNT experiment (with satellite AD). First, the

TABLE 1. The configuration of 11 HWRF experiments. For each experiment, there are twenty 5-day forecast cycles, initializing every 6 h from 1800 UTC 22 Oct to 1200 UTC 27 Oct 2012.

Expt	Obs assimilated	HWFR D-1 grid points
SMA1	Conventional data only	189 × 406
CNT1		216 × 432
BIG1		243 × 460
BIG2		270 × 486
BIG3		297 × 512
WSMA	Conventional and all satellite data (AMSU-A, AMSU-B, MHS, ATMS, AIRS, HIRS, SEVIRI, GOES Sounder)	189 × 406
WCNT		216 × 432
WBIG1		243 × 460
WBIG2		270 × 486
WBIG3		297 × 512
NSND	Conventional and all satellite data, excluding GOES Sounder	216 × 432

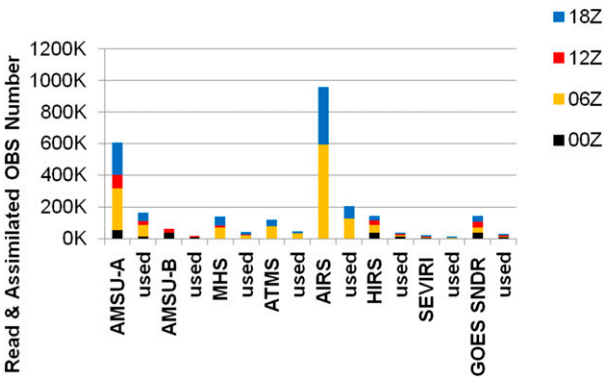

FIG. 2. The satellite observation numbers read in and assimilated (used) by the GSI/HWRF system for each sensor within 1-day-cycle experiments on 23 Oct 2012 over WCNT's D-1 region.

wind fields of the WCNT analysis in domain 2 were transferred to a cylindrical coordinate system with respect to the hurricane center at each time. Second, the FFT was performed for the tangential wind along the azimuthal direction at all radii and for all vertical levels. By averaging the magnitudes of wavenumbers 0–3 from 0000 UTC 24 October (when the hurricane eye began developing) to 1200 UTC 27 October 2012 (the last GSI analysis time), we examined the general pattern of Hurricane Sandy. As shown in Fig. 3, the magnitude of wavenumber 0 exhibits a typical hurricane tangential wind structure, which increases quickly from zero at storm center to its peak at the radius of maximum wind (RMW) around 75 km and then gradually decreases as the radius increases. The shapes of the wavenumber-0–3 magnitudes are similar to that found during Hurricane Gloria by Shapiro and Montgomery (1993), although there are some differences, mainly in wavenumber 0. Note that the RMW of Hurricane Gloria (1985) is smaller than that of Hurricane Sandy, and the magnitude of the wavenumber-0 tangential wind in Hurricane Gloria is about twice as strong as what was calculated for Hurricane Sandy. This is because Sandy was a larger category-3 (maximum wind of 115 mi h^{-1}) storm and the time-averaged results are given in Fig. 3a, while Hurricane Gloria was a much more intense and compact category-4 storm with maximum winds of 145 mi h^{-1}.

By examining the time series of the tangential wind wavenumber-1 structure in the WCNT experiment (Fig. 3b), we can roughly divide the studied time into two regimes. From 1800 UTC 22 October to 0600 UTC 25 October, and after 0000 UTC 27 October, the tangential wind wavenumber-1 magnitudes are less than 4 m s^{-1}, and therefore the storm is determined to have a dominated axisymmetric structure. For the time period from 1200 UTC 25 October to 1800 UTC 26 October, the wavenumber-1 magnitudes are bigger than 4 m s^{-1}. This is the time period when Hurricane Sandy showed strong asymmetric features. The time evolution of the wavenumber-1 features is also examined for the wind field from the CNT1 experiment (Fig. 3c). It is found that the magnitudes are smaller than those in WCNT during most times, especially for the period when Sandy has strong asymmetries. Therefore, the assimilation of satellite radiance data can produce analysis fields with more asymmetric structures under a shear environment.

Figure 4 shows AVHRR observations and two vertical cross sections of the warm core anomalies calculated from the GSI-analyzed temperature fields of the WCNT experiments when Hurricane Sandy was in the midst of its axisymmetric and asymmetric stages. At 0600 UTC Oct 25 October, Sandy was at its highest intensity stage (category 3), with a minimum sea level pressure (MSLP) of 957 hPa and maximum sustained winds of 110 mi h^{-1}. The AVHRR Imager (about 2.5 h later) shows an axisymmetric cloud pattern near the hurricane eyewall region. A maximum warm core anomaly of about 11 K can be found at the 400-hPa level in Fig. 4b. This is a typical warm core structure that can be found in an axisymmetric tropical cyclone, and the warm core extends up to the 200-hPa level. After just 1 day (0600 UTC Oct 26), Sandy weakened to a category 1 hurricane with an MSLP of 968 hPa and maximum sustained winds of 85 mi h^{-1}. Sandy's structure became more asymmetric, and the strong convection was concentrated on the northeast side of the storm (Fig. 4c). The maximum warm core anomaly was reduced to about 9 K and went down to the 550-hPa level. This height is much lower than that of a typical tropical cyclone, which is around the 250-hPa level (Zhu et al. 2002). The warm core also

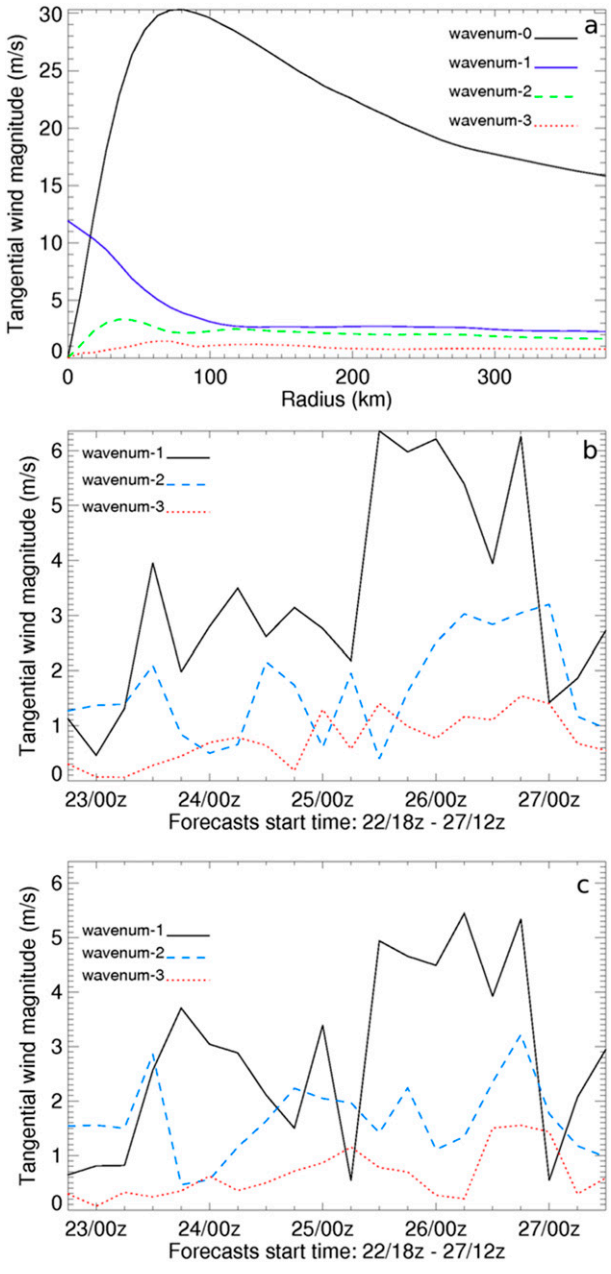

FIG. 3. (a) The magnitudes of wavenumbers 0–3 of WCNT's tangential winds averaged over the levels from 700 hPa to the surface during 0000 UTC 24 Oct–1200 UTC 27 Oct 2012. (b) The time series of the magnitudes of wavenumbers 1–3 of WCNT's tangential winds averaged over radii of 63–117 km across the levels from 700 hPa to the surface. (c) As in (b), but from the CNT1 analysis.

showed asymmetric structure and tilted westward, toward the less cloudy downward motion region.

Figure 5a shows the GSI-analyzed temperature field over HWRF's D-2 region with the assimilation of satellite radiance data (WCNT experiment) at 0600 UTC 26 October 2012. The differences between the GSI analyses with and without the assimilation of satellite radiance data (WCNT − CNT1) show that the WCNT experiment provides more asymmetric structure for the temperature field (Fig. 5b). There is an about a 1–2-K cold temperature anomaly area in the region to the northeast of the storm center near 27.5°N, 72.5°W, which likely corresponds to the strong convective rainband in this region (Fig. 4c). Usually, this kind of cold anomaly can be found at midtroposphere levels within convective regions (Zhu et al. 2002).

In the meantime, the assimilation of satellite data also changes the GSI-analyzed wind field, especially near the hurricane core region. Figure 6a shows that there was a strong mid- to upper-level trough in the northwest part of the environmental region near 450-hPa height, which interacted with Sandy later (Blake et al. 2013). It was found that there was no noticeable difference between the U components of the wind fields with and without the assimilation of satellite data in the environmental region (Fig. 6b), which indicated that GSI control analysis (CNT1) already captured the general environmental flow patterns. The assimilation of satellite data led to noticeable wind changes, mostly near the hurricane center area. The westward winds 140 km west of the storm center were increased in the WCNT experiment (Fig. 6c). There was also a long band of increasing V component along the north side of the storm core region (Fig. 6d). These increments of the winds in the WCNT experiment directly contributed to the storm's northwestward movement during the first 12 h of the forecast (see Fig. 7c and discussion in the next section). It is likely that the ability to capture these asymmetric features by assimilating satellite data enabled the WCNT experiment to produce a better track forecast at this time compared with the CNT1 experiment.

b. *Track forecasts with and without satellite data assimilation*

One of the more challenging aspects of the Hurricane Sandy track forecast was whether the storm would hook westward toward the U.S. mainland, and where it would make landfall along the Eastern Seaboard. Although most major NWP centers predicted the landfall area reasonably well 5 days in advance, the ECMWF forecast gave an early indication with 7–8-day lead time that the storm would take a sharp westward turn and make landfall in the mid-Atlantic states, which attracted considerable attention within and beyond the weather enterprise community (McNally et al. 2014).

To investigate the impact of satellite data assimilation on the HWRF track forecast, a comparison between the CNT1 and WCNT experiments was performed. Figure 7

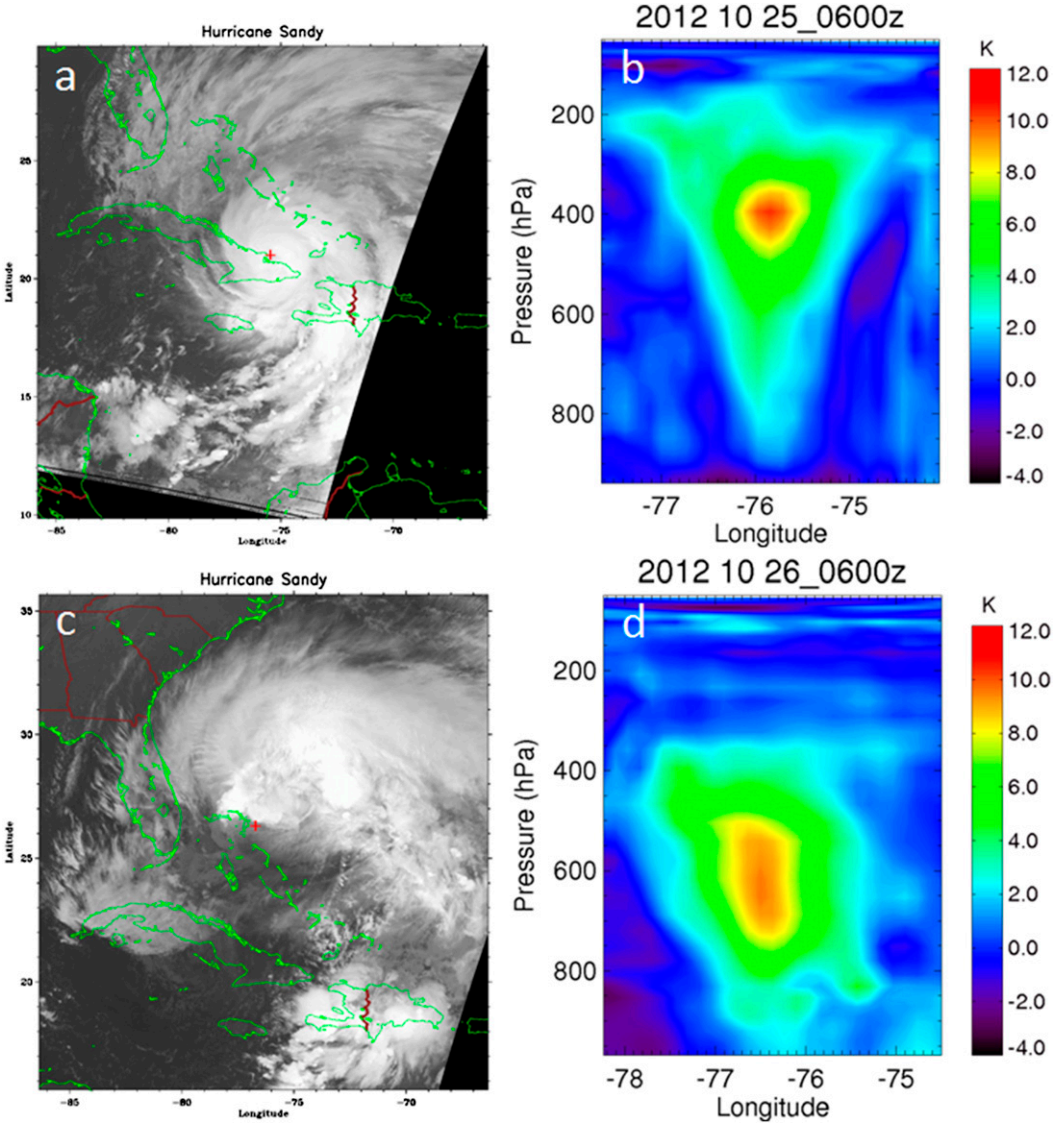

FIG. 4. The AVHRR channel 4 observations at (a) 0836 UTC 25 Oct and (c) 0825 UTC 26 Oct 2012, and the GSI analysis temperature field of the vertical cross sections of warm core anomaly at (b) 0600 UTC 25 Oct and (d) 0600 UTC 26 Oct 2012. The storm center is denoted with a red plus sign.

shows the comparison of the experiments at four different initial times. These times represent the different developmental stages of Hurricane Sandy: 1800 UTC 22 October, 0600 UTC 25 October, 0600 UTC 26 October, and 1200 UTC 27 October. It can be seen that at the beginning and the end of the experiments (Figs. 7a,d), the track forecasts with (WCNT) and without (CNT1) the assimilation of satellite data are very similar, and there are only minor differences for the 2- and 3-day forecasts. For the experiments starting at 0600 UTC 25 October, the WCNT forecast is a little better than that of the CNT1 forecast after day 1. Large differences can be found for the 0600 UTC 26 October forecast cycle. The track predicted by the WCNT experiment follows the best track closely, while the CNT1 track fails to turn sharply westward after day 3, forecasting landfall about 130 km to the northeast of where Sandy actually made landfall. As shown in Figs. 5 and 6, at this time, the GSI analysis with satellite DA improved the initial conditions mostly near Sandy's core region and not in the environmental region. We also computed the mean steering flows of the GSI analysis fields and found that there was little change for the steering flows with and without satellite data assimilation. We believe that satellite DA did not improve the steering flow directly in this forecast cycle. It was the interaction between the

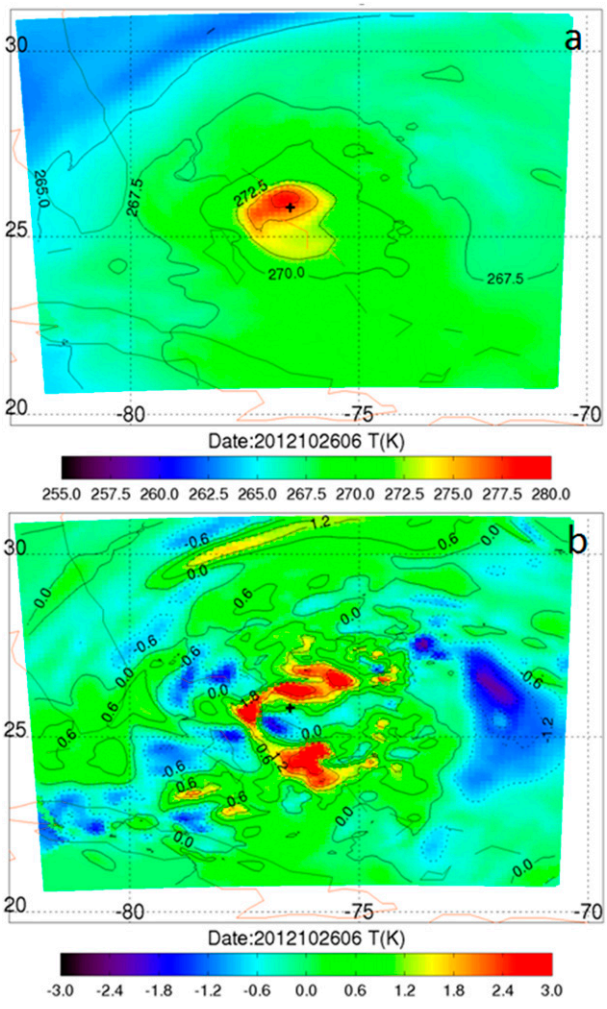

FIG. 5. (a) The temperature field of GSI analysis for experiment WCNT. (b) The temperature differences between experiments WCNT and CNT1 (WCNT − CNT1), over HWRF's D-2 sigma level 21 (close to 450 hPa) at 0600 UTC 26 Oct 2012. The storm center is indicated with a plus sign.

modified storm asymmetrical features and the environmental flow that led to the improvement of the storm track forecast. Brennan and Majumdar (2011) suggested that the correction of multiple sources of errors in the initial states, including the tropical cyclone itself and its near and far environments, in conjunction with reliable ensemble forecasts would lead to improved forecasts of Hurricane Ike's (2008) track. Möller and Shapiro (2005) indicated that the spinup of preexisting asymmetric features could have a substantial influence on the character of the convective activity and have a substantial lasting consequence for the intensification of a hurricane. Furthermore, Wang and Holland (1996) demonstrated that the asymmetric divergent flow associated with the convective asymmetries affected the vortex motion by deflecting the vortex to the region with maximum convection in a vertically sheared environment.

Figure 8 shows the comparison of the track forecast errors for all 20 HWRF forecast cycles for the CNT1 and WCNT experiments between 1800 UTC 22 October and 1200 UTC27 October. The dashed black line indicates the improvement in the track forecast errors after the assimilation of satellite data. It is found that the times with the large improvements to the track forecast are at 1800 UTC 24 October, 1200 UTC 25 October, and 0600–1800 UTC 26 October. Coincidentally, most of these times are within the time period when Hurricane Sandy encountered an upper-level trough coming from northwest and experienced strong asymmetric structures (Fig. 3b). There are also many other factors that can affect the improvement seen in the track forecast, even with the assimilation of satellite data. For example, when Sandy showed strong asymmetric structures at 1800 UTC 25 October and 0000 UTC 26 October, the control experiments (CNT1) produced very small forecast errors (about 50 n mi; 1 n mi = 1.852 km) at these times. This means that, at this time, the initial conditions in CNT1 were already good enough, and there was little room for the satellite AD experiments (WCNT) to make further improvement (Fig. 8). One reasonable speculation from this case study is that the analyses with the assimilation of satellite data in the WCNT experiments capture the asymmetric structures near the storm and its ambient environmental area, which then results in a better track forecast. This result indicates that one favored time for satellite data assimilation to make a positive impact on the hurricane track forecasts is when a storm has strong asymmetric features near the core region and its ambient environment, because the storm asymmetric patterns, as well as the placement of troughs and ridges in the environment, can be easily detected with satellite observations (Weber 1999).

A composite figure of the track forecast from a series of forecast cycles, or the track forecast envelope, also illustrates the differences between the CNT1 and WCNT track forecasts. The 5-day track forecast envelopes, consisting of seven CNT1 and WCNT experiments initialized from 1800 UTC 25 October to 1200 UTC 27 October, are shown in Figs. 9a and 9b Assessment of the individual track forecasts shows only minor differences between the CNT1 and WCNT experiments. However, the envelope of the CNT1 track is broader than that for the WCNT experiment after 3.5 days, and the standard deviation of the track errors is also larger for the CNT1 experiment after 4 days. This comparison indicates that there is more uncertainty for Sandy's track forecast without the assimilation of satellite data. In other words,

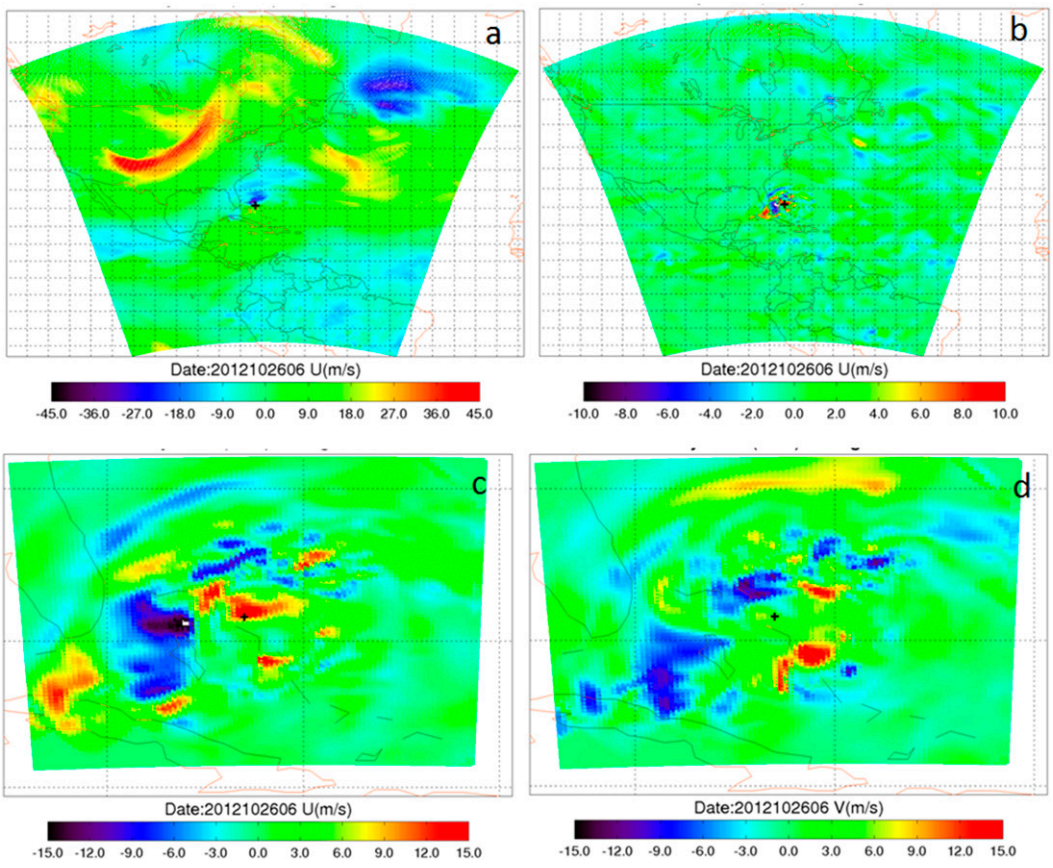

FIG. 6. The GSI-analyzed wind fields over sigma level 21 (close to 450 hPa) at 0600 UTC 26 Oct 2012 for (a) the *U* component for experiment CNT1 over HWRF's D-1. (b) The difference among the *U* components between experiments WCNT and CNT1 (WCNT − CNT1) over HWRF's D-1. (c) As in (b), but over D-2. (d) As in (c), but for the *V* component. The storm center is indicated with a plus sign.

the satellite DA provides more consistent initial conditions for the HWRF model and leads to the reduction of track forecast uncertainty.

To investigate the impact of just the GOES Sounder data on the HWRF forecasts, the NSND experiment was performed with all satellite data assimilated except for the *GOES-13/15* Sounder observations (radiances and the derived atmospheric motion vectors). By averaging all 20 cycles of the HWRF 5-day simulations, the comparisons of the forecast errors against the best track for the CNT1, WCNT, and NSND experiments are given in Fig. 10, along with the errors of the operational global GFS forecasts. Comparing with the control run, there is small improvement seen in the track forecast errors for both the WCNT and NSND experiments (Fig. 10a) after 3.5 days. It is apparent that the assimilation of all satellite data (WCNT) has a positive impact on Sandy's MSLP forecasts (Fig. 10b). For the NSND experiment, the positive impact on the MSLP forecast shown in WCNT is reduced with the removal of the GOES Sounder data. However, there is no significant improvement seen in the maximum sustained wind forecasts for the WCNT and NSND experiments (Fig. 10c). In general, the benefit of the assimilation of all satellite data and the contribution from the GOES Sounder observations are easy to identify in the MSLP forecasts, although there are mixed signals at lead times from 72 to 96 h. This is because a hurricane center pressure (mass field) is a value that mainly relates to the intensity of the whole storm system, and its variation is smooth. On the other hand, the maximum sustained wind is associated with individual convective cells, making it very much localized and highly variable in time and therefore difficult to predict.

Finally, we note that the HWRF track forecast errors (with or without satellite data assimilation) are larger than the operational GFS forecasts (Fig. 10a). It is well known that global NWP provides better tropical cyclone track forecasts than regional models, because the environmental steering flow can be better predicted by the global model (Gall et al. 2013; Tallapragada et al. 2015,

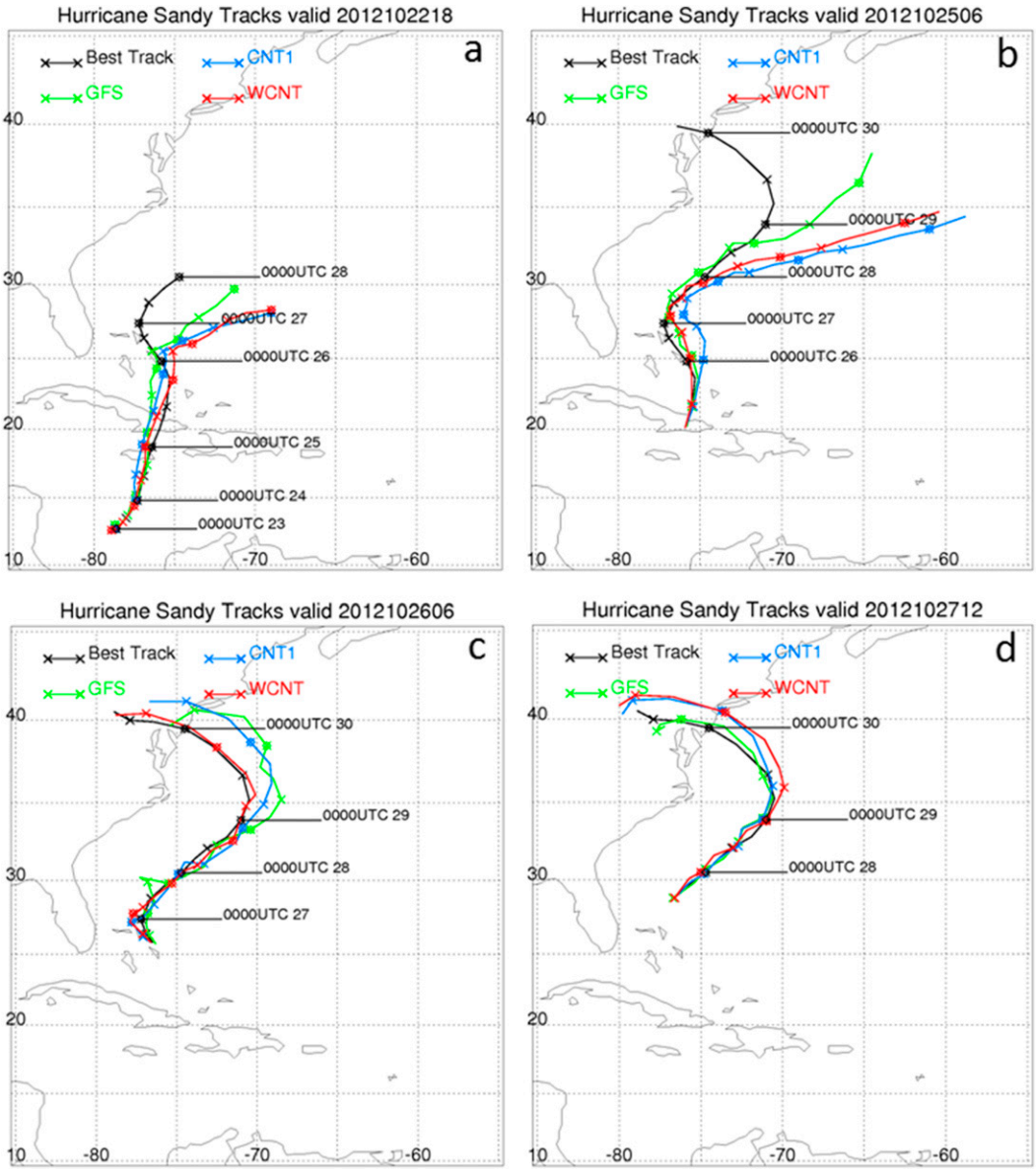

FIG. 7. Five-day track forecasts of Hurricane Sandy made by the CNT1 and WCNT experiments, and also compared with NCEP GFS forecast and best-track results, starting at (a) 1800 UTC 22 Oct, (b) 0000 UTC 25 Oct, (c) 0600 UTC 26 Oct, and (d) 1200 UTC 27 Oct 2012. The storm centers are indicated at a 12-h interval at 0000 UTC with diamond symbols and at 1200 UTC with exes.

2016a). However, because of the lower spatial resolution and relatively simple physics schemes, the intensity forecasts (MSLP and maximum wind) from GFS are not as good as those of HWRF (Figs. 10b,c), mainly within 72-h lead times.

c. *Comparison the forecast errors of satellite DA and LBC*

As mentioned in the introduction, the LBCs are always important considerations for regional forecast models. To evaluate the LBCs' impact on tropical cyclone track forecasts, eight more experiments were conducted with variations in the HWRF D-1 size. By varying the HWRF D-1 size, the LBCs obtained from the global model are changed. Since the D-1 lateral boundary data comes from the more realistic environmental flow of the global model, our hypothesis is that a smaller D-1 size can provide a better constraint for a regional model forecast. On the other hand, the total volumes of satellite data assimilated by GSI when

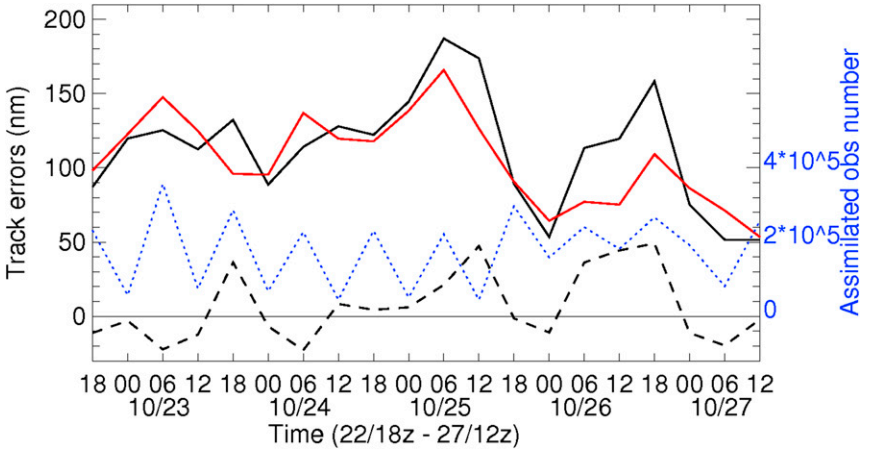

FIG. 8. The time series of the assimilated satellite data volume and the averaged track forecast errors for 20 cycles initiated from 1800 UTC 22 Oct to 1200 UTC 27 Oct 2012. The dotted blue line is the assimilated satellite data volume during these 20 cycles. The solid black and red lines are the averages of 0–126-h forecast track errors from the CNT1 and WCNT experiments, respectively. The dashed black line is the difference (CNT1 − WCNT) among the track errors between the CNT1 and WCNT experiments.

extending the LBCs are increased by 49.5% and 55.4%, respectively, as the D-1 size changes from CNT1 to BIG3 (as shown in Fig. 1), which should provide positive impacts on the regional model forecasts.

Figure 11a shows the average track error from the 20 forecast cycles for lead times of 24–120 h, as a function of D-1 size, using the best track as a reference. In general, there is not much difference between the forecast errors within the first 3 days when changing the HWRF D1 size, for both experiments with and without the assimilation of satellite data. For forecasts longer than 4 days, the track errors with the assimilation of satellite data are smaller than those without the assimilation of satellite data, which confirms the finding in the previous section. However, it is found that the track errors show increased sensitivity to the domain size. Even with the assimilation of satellite data (dashed lines), the track forecast error becomes larger with an increase in domain size for the day-4/5 forecasts. The errors due to the increase in D-1 size dominate any reduction in error realized by assimilating more satellite observations. It is believed that the larger domain increases the internal variability of the model fields, such that the deviation of the forecast for the large-scale flow of the LBCs becomes strong.

Another way of assessing the impact of the LBCs is by comparing Figs. 11a and 11b. Instead of calculating the track error against the best track, the errors are computed with respect to GFS-forecasted tracks, as provided in Fig. 11b. This result shows that the track errors with respect to the GFS forecasts are about half of the magnitude of the errors when verifying against the best track (Fig. 11a), which implies that the simulated storm track tends to follow the steering flow provided by the LBCs. Although the magnitudes of the track errors are very different when compared with the best track and GFS forecasts, the patterns shown in Figs. 11a,b are similar. The results with both calculations show that the smallest D-1 sized lead to the best track forecasts. This indicates that the LBCs with realistic environmental flow information can provide better constraints on smaller-domain regional forecasts. Similar findings were presented by Steeneveld et al. (2015), who indicated that the simulation of radiation fog with the smallest WRF model domain better captures reality.

When examining the intensity forecasts, it is found that there are small or random changes for the MSLP and maximum wind forecast errors with respect to the domain-1 size changes (not shown). This indicates that the intensity forecasts are not affected by the changes in the domain-1 size. In addition, we can also see that the overall intensity forecast errors are reduced after satellite data assimilation, similar to the results found in Figs. 10 and 11.

4. Summary and discussion

Satellite data assimilation and lateral boundary condition impacts on the HWRF model forecast of Hurricane Sandy in October 2012 were investigated in this study. Two parallel experiments were designed to evaluate the impacts of the assimilation of all satellite data, producing 5-day forecasts from 20 HWRF cycles

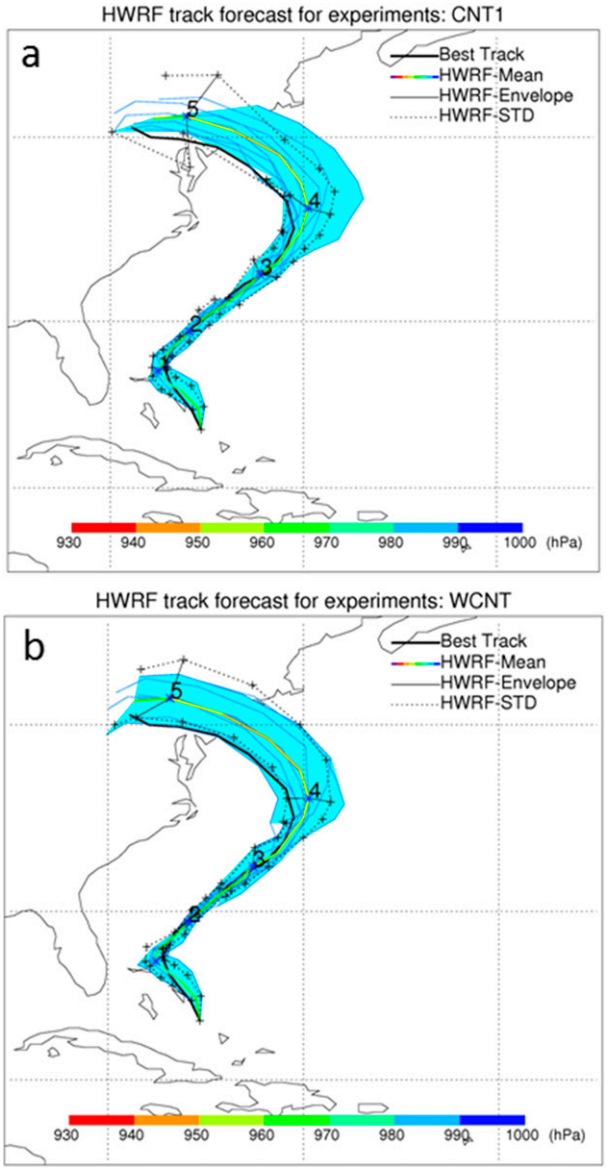

FIG. 9. The 5-day forecast tracks with the model initialized every 6 h from 1800 UTC 25 Oct to 1200 UTC 27 Oct 2012 for experiments (a) CNT1 and (b) WCNT. The light blue highlighted region is the envelope of tracks predicted by seven experiments. The eight thin blue curves are the tracks of eight forecast cycles; the thick colored curve is the averaged mean track of the eight cycles, and the color scale denotes the MSLP; the two dotted curves are the standard deviation of the eight tracks.

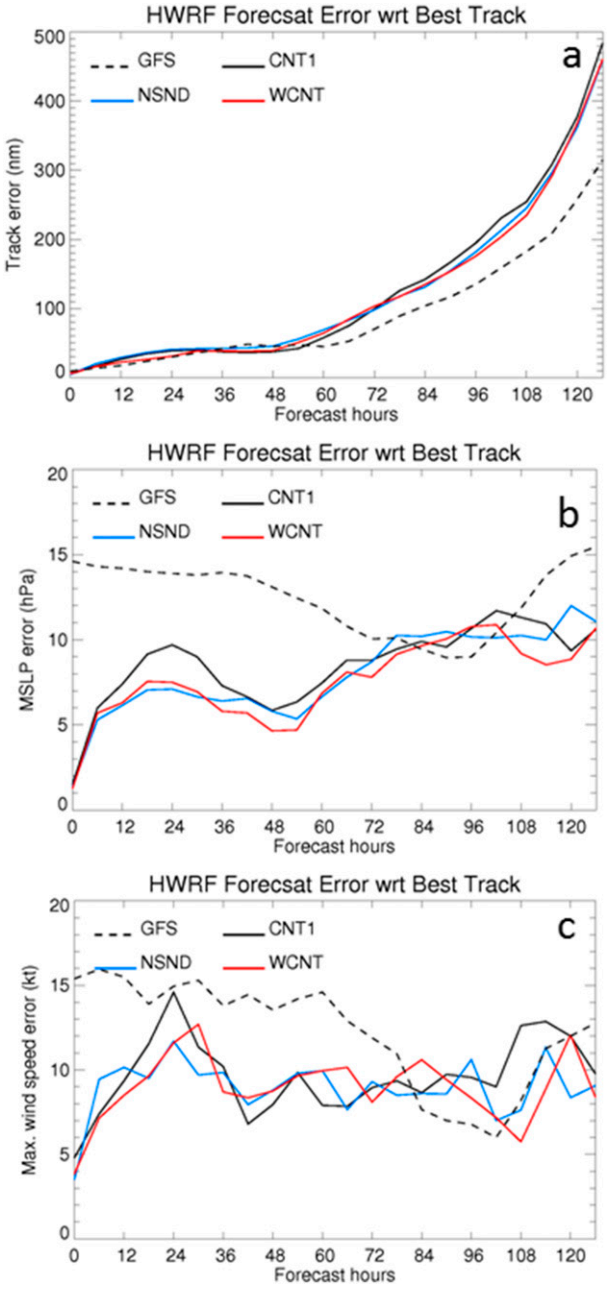

FIG. 10. Comparison the forecast errors of (a) track, (b) MSLP, and (c) maximum wind, from the CNT1, WCNT, and NSND experiments, as well as the operational global GFS forecast, averaged over 20 HWRF cycles for each experiment.

spanning from 1800 UTC 22 October to 1200 UTC 27 October, at 6-h intervals. One set of experiments assimilated only conventional observations, and the second set assimilated both conventional and satellite observations. The evolution of the magnitude of the wavenumber-1 tangential wind and the warm core anomaly structures showed that there were two regimes in Hurricane Sandy's life cycle (i.e., axisymmetric and asymmetric stages). The GSI analyses with the assimilation of satellite data captured the asymmetric structures near the hurricane eyewall and its ambient environment, which led to better track forecasts. Without satellite data assimilation, there was larger uncertainty among the track forecasts for Sandy when comparing the composite

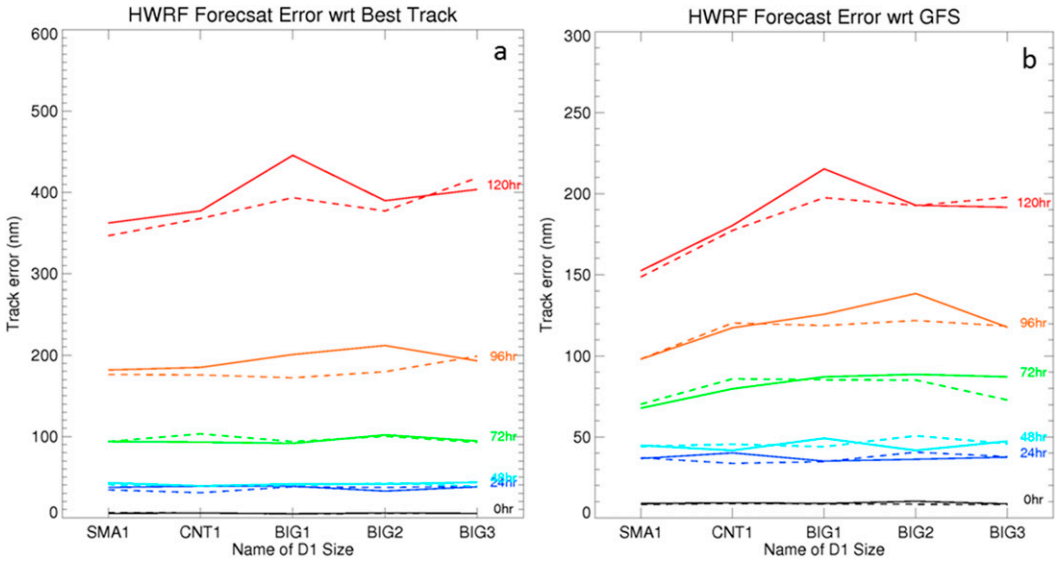

FIG. 11. The 20 forecast cycles averaged forecast track errors w.r.t. (a) the best track and (b) the GFS operational forecast from five different domain-size experiments. The dashed and solid curves are for the experiments with and without the assimilation of satellite data, respectively. The color of the line indicates the forecast hours.

forecast track envelopes. This result indicates that satellite data assimilation can improve the representation of a hurricane's asymmetry for the initial conditions, especially in a shear environment and then lead to a better track forecast.

Another experiment was performed with the removal of all GOES Sounder data from all satellite data assimilation experiments. By removing the GOES Sounder data, there was a large negative impact realized on the MSLP forecast. However, there was only slight positive impact on the track forecast after 3.5 days and almost no impact on the maximum sustained wind forecasts for both all satellite data assimilation experiments and GOES Sounder denial experiments. This is mainly because a hurricane center pressure is a value that primarily relates to the mass balance of the tropical system as a whole, and its variation is smooth. On the other hand, the maximum sustained wind is largely associated with individual convective cells within the system that are highly localized and have large variance on short time and spatial scales, making it more difficult to accurately predict the results.

By modifying the HWRF domain size, the impacts from the lateral boundary conditions as well as the inclusion of satellite data assimilation on the track and intensity forecasts were also assessed and compared. For day-1–3 track forecasts verified against the best track, it was shown that the increase in domain size had little impact on the overall HWRF performance, even with the assimilation of satellite data, where increasing the domain-1 size from 189 × 406 to 297 × 512 grid points increased the total volume of satellite data points assimilated by GSI by 55.4%. At the longer lead times (e.g., day 4/5), the increase in the domain-1 size from 189 × 406 to 297 × 512 grid points shows a significant increase in the forecast track error and dominates any improvement found in track error when including the satellite data in the assimilation. The track errors, when verified against GFS forecasts, were half of those found when verified against the best track, which implied that the simulated storm track tends to follow the steering flow provided by the lateral boundary conditions. However, the trend in the results when increasing the domain size was similar to those determined when verifying against the best track, both with and without satellite data assimilation. It is believed that the lateral boundary conditions containing realistic environmental flow information can provide a better constraint when a smaller domain is defined. Specification of a larger domain increases the internal variability of the regional model, such that the deviation of the forecast from the large-scale features provided by the lateral boundary conditions becomes stronger. This study emphasized the challenges associated with the evaluation of satellite data impacts on regional numerical weather prediction due to the influence of lateral boundary conditions.

It should be noted that just one case study was performed for Hurricane Sandy, which was a large hurricane. The impact of model domain size on storm track could be different for a smaller storm. Additional cases

studies are necessary to evaluate the conclusions in this study.

The HWRF model used in this case study is FY13 v3.5a. Recently, Tallapragada et al. (2016b) reported that the evaluation of HWRF FY14 upgrades showed improvements in track and intensity forecasts, with the track errors comparable to the best-performing GFS model, and preimplementation tests showing reductions in track and intensity forecast errors when the HWRF FY15 configuration was tested. In addition to many physics upgrades since HWRF FY13, there are also several other important implementations of the HWRF infrastructure. In HWRF FY14, the vertical resolution was increased from 42 to 61 levels, and the model top was extended from 50 to 2 hPa, which allowed for more satellite data to be ingested. The inner two domains, D-2 and D-3, were increased by 20% and 10%, respectively. In HWRF FY15, the model resolutions were increased from 27/9/3 km to 18/6/2 km for the three nested domains. The GSI analysis was run on D-2, and then the analysis increment was added to D-3. Each of these upgrades have made certain contributions to the improvement of track forecasts.

This result indicates that without changing the domain-1 size (or the LBCs), the track forecast error can be improved by increasing satellite data usage, changing the domain resolutions and the inner two domain sizes, and using compatible physics schemes. In this study, we compared the impacts of satellite DA and LBCs, and found that the uncertainty in the LBCs could dominate the benefits from assimilating an increased volume of satellite observations. The impacts of the outer domain size on the track forecasts may be smaller in the new HWRF model after all of these upgrades. It is desired to perform more tests to investigate which implementation in the new HWRF model is critical, or to learn if all of the upgrades work together for the improvement of the track forecasts. No satellite data are assimilated in domain 1 of the HWRF FY14 or FY15 systems. Tallapragada et al. (2016b) indicated that the GSI system will be used in the future to improve the initial analyses for all HWRF domains. This study provided a preliminary test result of the impacts of satellite DA over HWRF's D-1.

Acknowledgments. The views expressed in this publication are those of the authors and do not necessarily represent those of NOAA. Dr. Krishna Kumar helped to obtain the FY13 HWRF model from DRT trunk. We thank Drs. Banglin Zhang, Qingfu Liu, and Mingjing Tong at NOAA/EMC for their help and productive discussion in using HWRF. This work was supported by NOAA/NESDIS (Grant 12142070).

REFERENCES

Anderson, J. L., 2001: An ensemble adjustment Kalman filter for data assimilation. *Mon. Wea. Rev.*, **129**, 2884–2903, doi:10.1175/1520-0493(2001)129<2884:AEAKFF>2.0.CO;2.

Blake, E. S., T. B. Kimberlain, R. J. Berg, J. P. Cangialosi, and J. L. Beven II, 2013: Tropical cyclone report Hurricane Sandy. National Hurricane Center Rep. AL182012, 157 pp. [Available online at http://www.nhc.noaa.gov/data/tcr/AL182012_Sandy.pdf.]

Bouttier, F., and G. Kelly, 2001: Observation-system experiments in the ECMWF 4D-Var data assimilation system. *Quart. J. Roy. Meteor. Soc.*, **127**, 1469–1488, doi:10.1002/qj.49712757419.

Brennan, M. J., and S. J. Majumdar, 2011: An examination of model track forecast errors for Hurricane Ike (2008) in the Gulf of Mexico. *Wea. Forecasting*, **26**, 848–867, doi:10.1175/WAF-D-10-05053.1.

Chikhar, K., and P. Gauthier, 2015: On the effect of boundary conditions on the Canadian Regional Climate Model: Use of process tendencies. *Climate Dyn.*, **45**, 2515–2526, doi:10.1007/s00382-015-2488-2.

Galarneau, T. J., C. A. Davis, and M. A. Shapiro, 2013: Intensification of Hurricane Sandy (2012) through extratropical warm core seclusion. *Mon. Wea. Rev.*, **141**, 4296–4321, doi:10.1175/MWR-D-13-00181.1.

Gall, R., J. Franklin, F. Marks, E. N. Rappaport, and F. Toepfer, 2013: The Hurricane Forecast Improvement Project. *Bull. Amer. Meteor. Soc.*, **94**, 329–343, doi:10.1175/BAMS-D-12-00071.1.

Joo, S., J. Eyre, and R. Marriott, 2013: The impact of MetOp and other satellite data within the Met Office global NWP system using an adjoint-based sensitivity method. *Mon. Wea. Rev.*, **141**, 3331–3342, doi:10.1175/MWR-D-12-00232.1.

Kleist, D. T., D. F. Parrish, J. C. Derber, R. Treadon, W.-S. Wu, and S. Lord, 2009: Introduction of the GSI into the NCEP Global Data Assimilation System. *Wea. Forecasting*, **24**, 1691–1705, doi:10.1175/2009WAF2222201.1.

Larsen, M. A., P. Thejll, J. H. Christensen, J. C. Refsgaard, and K. H. Jensen, 2013: On the role of domain size and resolution in the simulations with the HIRHAM region climate model. *Climate Dyn.*, **40**, 2903–2918, doi:10.1007/s00382-012-1513-y.

Liu, Q., X. Zhang, S. Trahan, and V. Tallapragada, 2012: Extending operational HWRF initialization to triple-nest HWRF system. *30th Conf. on Hurricanes and Tropical Meteorology*, Ponte Vedra Beach, FL, Amer. Meteor. Soc., 14A.6. [Available online at https://ams.confex.com/ams/30Hurricane/webprogram/Paper204853.html.]

Magnusson, L., J.-R. Bidlot, S. T. K. Lang, A. Thorpe, N. Wedi, and M. Yamaguchi, 2014: Evaluation of medium-range forecasts of Hurricane Sandy. *Mon. Wea. Rev.*, **142**, 1962–1981, doi:10.1175/MWR-D-13-00228.1.

McNally, T., M. Bonavita, and J.-N. Thépaut, 2014: The role of satellite data in the forecasting of Hurricane Sandy. *Mon. Wea. Rev.*, **142**, 634–646, doi:10.1175/MWR-D-13-00170.1.

Möller, J. D., and L. J. Shapiro, 2005: Influences of asymmetric heating on hurricane evolution in the MM5. *J. Atmos. Sci.*, **62**, 3974–3992, doi:10.1175/JAS3577.1.

Nadeem, I., and H. Formayer, 2015: Sensitivity studies of high-resolution RegCM3 simulations of precipitation over the European Alps: The effect of lateral boundary conditions and domain size. *Theor. Appl. Climatol.*, **126**, 617–630, doi:10.1007/s00704-015-1586-8.

Pu, Z., X. Li, and E. J. Zipser, 2009: Diagnosis of the initial and forecast errors in the numerical simulation of the rapid intensification of Hurricane Emily (2005). *Wea. Forecasting*, **24**, 1236–1251, doi:10.1175/2009WAF2222195.1.

Schwartz, C. S., Z. Liu, Y. Chen, and X.-Y. Huang, 2012: Impact of assimilating microwave radiances with a limited-area ensemble data assimilation system on forecasts of Typhoon Morakot. *Wea. Forecasting*, **27**, 424–437, doi:10.1175/WAF-D-11-00033.1.

Shapiro, L., and M. T. Montgomery, 1993: A three-dimensional balance theory for rapidly rotating vortices. *J. Atmos. Sci.*, **50**, 3322–3334, doi:10.1175/1520-0469(1993)050<3322:ATDBTF>2.0.CO;2.

Simmons, A. J., and A. Hollingsworth, 2002: Some aspects of the improvement in skill of numerical weather prediction. *Quart. J. Roy. Meteor. Soc.*, **128**, 647–677, doi:10.1256/003590002321042135.

Steeneveld, G. J., R. J. Ronda, and A. A. M. Holtslag, 2015: The challenge of forecasting the onset and development of radiation fog using mesoscale atmospheric models. *Bound.-Layer Meteor.*, **154**, 265–289, doi:10.1007/s10546-014-9973-8.

Tallapragada, V., C. Kieu, Y. Kwon, S. Trahan, Q. Liu, Z. Zhang, and I. Kwon, 2014: Evaluation of storm structure from the operational HWRF model during 2012 implementation. *Mon. Wea. Rev.*, **142**, 4308–4325, doi:10.1175/MWR-D-13-00010.1.

——, and Coauthors, 2015: Forecasting tropical cyclones in the western North Pacific basin using the NCEP operational HWRF: Real-time implementation in 2012. *Wea. Forecasting*, **30**, 1355–1373, doi:10.1175/WAF-D-14-00138.1.

——, and Coauthors, 2016a: Forecasting tropical cyclones in the western North Pacific basin using the NCEP operational HWRF Model: Model upgrades and evaluation of real-time performance in 2013. *Wea. Forecasting*, **31**, 877–894, doi:10.1175/WAF-D-14-00139.1.

——, and Coauthors, 2016b: Hurricane Weather Research and Forecasting (HWRF) Model: 2015 scientific documentation. NCAR Tech. Note NCAR/TN-522+STR, 122 pp., doi:10.5065/D6ZP44B5.

Wang, Y., and G. J. Holland, 1996: Tropical cyclone motion and evolution in vertical shear. *J. Atmos. Sci.*, **53**, 3313–3332, doi:10.1175/1520-0469(1996)053<3313:TCMAEI>2.0.CO;2.

Warner, T. T., R. A. Peterson, and R. E. Treadon, 1997: A tutorial on lateral boundary conditions as a basic and potentially serious limitation to regional numerical weather prediction. *Bull. Amer. Meteor. Soc.*, **78**, 2599–2617, doi:10.1175/1520-0477(1997)078<2599:ATOLBC>2.0.CO;2.

Weber, H. C., 1999: A numerical study of tropical-cyclone structure: Quasi-stationary spiral bands. *Quart. J. Roy. Meteor. Soc.*, **125**, 811–836, doi:10.1002/qj.49712555504.

Wu, W.-S., D. F. Parrish, and R. J. Purser, 2002: Three-dimensional variational analysis with spatially inhomogeneous covariances. *Mon. Wea. Rev.*, **130**, 2905–2916, doi:10.1175/1520-0493(2002)130<2905:TDVAWS>2.0.CO;2.

Xu, J., S. Rugg, L. Byerle, and Z. Liu, 2009: Weather forecasts by the WRF-ARW Model with the GSI data assimilation system in the complex terrain areas of southwest Asia. *Wea. Forecasting*, **24**, 987–1008, doi:10.1175/2009WAF2222229.1.

Zapotocny, T. H., W. P. Menzel, J. A. Jung, and J. P. Nelson III, 2005: A four-season impact study of rawinsonde, GOES, and POES data in the Eta Data Assimilation System. Part II: Contribution of the components. *Wea. Forecasting*, **20**, 178–198, doi:10.1175/WAF838.1.

——, J. A. Jung, J. F. Le Marshall, and R. E. Treadon, 2007: A two-season impact study of satellite and in situ data in the NCEP Global Data Assimilation System. *Wea. Forecasting*, **22**, 887–909, doi:10.1175/WAF1025.1.

Zhang, X., T. S. Quirino, K.-S. Yeh, S. G. Gopalakrishnan, F. D. Marks Jr., S. B. Goldenberg, and S. Aberson, 2011: HWRFx: Improving hurricane forecast with high-resolution modeling. *Comput. Sci. Eng.*, **13**, 13–21, doi:10.1109/MCSE.2010.121.

Zhu, T., and F. Weng, 2013: Hurricane Sandy warm-core structure observed from Advanced Technology Microwave Sounder. *Geophys. Res. Lett.*, **40**, 3325–3330, doi:10.1002/grl.50626.

——, D.-L. Zhang, and F. Weng, 2002: Impact of the Advanced Microwave Sounding Unit measurements on hurricane prediction. *Mon. Wea. Rev.*, **130**, 2416–2432, doi:10.1175/1520-0493(2002)130<2416:IOTAMS>2.0.CO;2.